J. Shanghai Jiao Tong Univ. (Sci.), 2018, 23(5): 650-656
https://doi.org/10.1007/s12204-018-1994-x

Finite-Time Attitude Tracking Control of Spacecraft with Actuator Saturation

LIU Yueyang (刘岳洋), *HU Qinglei*[*] (胡庆雷), *GUO Lei* (郭　雷)
(School of Automation Science and Electrical Engineering, Beihang University, Beijing 100191, China)

Abstract: The attitude tracking control problem of a rigid spacecraft with actuator saturation is investigated in this paper. A finite-time attitude tracking control scheme is presented by incorporating sliding mode control (SMC) and adaptive technique. Specifically, a novel time-varying sliding mode manifold is first developed that aims at regulating the attitude tracking error to equilibrium point within a certain finite time. Moreover, it can be specified a priori by the designer according to the mission requirement. Subsequently, an adaptive controller is derived by using the SMC in conjunction with adaptive technique. The designed controller is capable of ensuring that the state trajectories reach to sliding regime within a finite time, and hence that attitude tracking error can converge to zero in a finite time with the aid of the developed sliding dynamics, despite the presence of exogenous disturbances, unknown inertia properties and saturation nonlinearities. Finally, the simulation experiments are carried out to demonstrate the effectiveness of the proposed control scheme.

Key words: time-varying sliding mode, finite-time convergence, input saturation, attitude tracking, spacecraft
CLC number: V 448.2　　**Document code:** A

0 Introduction

The attitude tracking control of a rigid spacecraft has attracted a great deal of interest during the past decades, owing to its extensive applications in aerospace engineering. In this direction, many advanced nonlinear control strategies have been proposed to improve the control performance, such as adaptive control[1], sliding mode control (SMC)[2-3], and H_∞ inverse optimal control[4]. Among them, SMC as an effective approach has been extensively applied to attitude tracking control of spacecraft, largely because of its rapid response and insensitivity to uncertain parameters and disturbances.

Although SMC is able to guarantee good control performance for spacecraft attitude tracking maneuvers, it can only provide infinite-time convergence in general. In practice, guaranteeing the convergence of the attitude tracking error to equilibrium point within a finite time is more desired for some high demanding real-time missions. Jin and Sun[5] presented an alternative solution to finite-time attitude tracking control by means of terminal SMC (TSMC). However, one caveat is that most of the existing TSMC schemes are discontinuous and have a singularity problem. Zou et al.[6] proposed a finite-time control scheme to overcome the singularity problems by terminal sliding mode and neural network technique.

Besides, control input saturation is also a practical problem that deserves more attention in the design of attitude tracking controller[7]. From a practical viewpoint, actuator saturation may give rise to undesirable performance degradation or lead to system instability. Analysis and design of attitude systems with input saturation nonlinearities were studied in Refs. [8-11]. Many finite-time attitude control methodologies with actuator saturation have been designed on the assumption that some system states are bounded. To date, finite-time control design for spacecraft applications with explicit consideration of actuator saturation is still an open problem.

In this paper, we address the problem of attitude tracking control with finite-time convergence for a rigid spacecraft subjected to input saturation and the presence of exogenous disturbances. A valid solution is presented by incorporating SMC and adaptive technique. Specifically and firstly, a novel time-varying sliding mode manifold is developed that aims at achieving the finite-time convergence of the attitude tracking error. Meanwhile, the discontinuity and singularity of TSMC are avoided. Subsequently, a special auxiliary system is introduced to overcome the input saturation. Then an

Received date: 2018-06-27
Foundation item: the National Natural Science Foundation of China (Nos. 61522301 and 61633003)
***E-mail:** huql_buaa@buaa.edu.cn

adaptive controller is derived, which is capable of ensuring that the state trajectories reach to sliding regime within a finite time, and hence that attitude tracking error can converge to zero in a finite time. It is shown that the control algorithm developed is robust against exogenous disturbances and adaptive to unknown inertia properties. In particular, by incorporating a novel time-varying forcing function into the sliding dynamics, the attitude tracking error is proven to converge to zero within a pre-determined time, and the terminal time as an explicit parameter can be specified a priori by the designer according to mission requirement. Finally, the effectiveness of the proposed control scheme is illustrated via simulation experiments.

1 Problem Formulation

1.1 Dynamic Model of Rigid Spacecraft

The finite-time attitude tracking task of a rigid spacecraft is focused in this paper, and the kinematic and dynamics equations of motion in terms as quaternion are describe by

$$\left.\begin{aligned}\dot{\boldsymbol{q}}_{\mathrm{v}} &= \frac{1}{2}(\boldsymbol{q}_{\mathrm{v}}^{\times} + \boldsymbol{q}_4\boldsymbol{I}_3)\boldsymbol{\omega}\\ \dot{q}_4 &= -\frac{1}{2}\boldsymbol{q}_{\mathrm{v}}^{\mathrm{T}}\boldsymbol{\omega}\end{aligned}\right\}, \tag{1}$$

$$\boldsymbol{J}\dot{\boldsymbol{\omega}} = -\boldsymbol{\omega}^{\times}\boldsymbol{J}\boldsymbol{\omega} + \boldsymbol{\tau} + \boldsymbol{T}_d, \tag{2}$$

where, $\boldsymbol{q} = [\boldsymbol{q}_{\mathrm{v}}^{\mathrm{T}} \quad q_4] \in \mathbb{R}^4$ denotes the attitude orientation of the rigid-body spacecraft with respect to an inertial frame, and $\boldsymbol{I}_3 \in \mathbb{R}^{3\times 3}$ denotes the identity matrix; $\boldsymbol{x}^{\times}$ represents a skew-symmetric matrix, and for $\forall \boldsymbol{x} = [x_1 \quad x_2 \quad x_3]$, $\boldsymbol{x}^{\times}$ is defined as

$$\boldsymbol{x}^{\times} = \begin{bmatrix} 0 & -x_3 & x_2 \\ x_3 & 0 & -x_1 \\ -x_2 & x_1 & 0 \end{bmatrix};$$

$\boldsymbol{\omega}$ denotes the angular velocity body-fixed frame of spacecraft in the body frame with respect to the inertial reference frame; $\boldsymbol{J} \in \mathbb{R}^{3\times 3}$ denotes the inertia matrix of spacecraft; $\boldsymbol{\tau}$ represents the control torque produced by the actuator; $\boldsymbol{T}_{\mathrm{d}} \in \mathbb{R}^3$ represents the external disturbance.

1.2 Relative Attitude Dynamics

In order to pursue the attitude tracking control problem, the error quaternion $\boldsymbol{q}_{\mathrm{e}} = \begin{bmatrix}\boldsymbol{q}_{\mathrm{ev}}^{\mathrm{T}} \\ q_{\mathrm{e4}}\end{bmatrix} \in \mathbb{R}^3 \times \mathbb{R}$ is given by

$$\boldsymbol{q}_{\mathrm{e}} = \boldsymbol{q} \otimes \boldsymbol{q}_{\mathrm{d}}^{*} = \begin{bmatrix} q_{\mathrm{d4}}\boldsymbol{q}_{\mathrm{v}} - q_4\boldsymbol{q}_{\mathrm{dv}} + \boldsymbol{q}_{\mathrm{v}}^{\times}\boldsymbol{q}_{\mathrm{dv}} \\ q_{\mathrm{d4}}q_4 + \boldsymbol{q}_{\mathrm{dv}}^{\mathrm{T}}\boldsymbol{q}_{\mathrm{v}} \end{bmatrix}, \tag{3}$$

where, $\boldsymbol{q}_{\mathrm{d}}^{*}$ is the conjugate quaternion of $\boldsymbol{q}_{\mathrm{d}}$, and $\boldsymbol{q}_{\mathrm{d}} = \begin{bmatrix}\boldsymbol{q}_{\mathrm{dv}}^{\mathrm{T}} \\ q_{\mathrm{d4}}\end{bmatrix} \in \mathbb{R}^3 \times \mathbb{R}$ denotes the desired attitude orientation; similarly, its motion is governed by $\dot{\boldsymbol{q}}_{\mathrm{dv}} = 0.5(\boldsymbol{q}_{\mathrm{dv}}^{\times} + q_{\mathrm{d4}}\boldsymbol{I}_3)\boldsymbol{\omega}_{\mathrm{d}}$ and $\dot{q}_{\mathrm{d4}} = -0.5\boldsymbol{q}_{\mathrm{dv}}^{\mathrm{T}}\boldsymbol{\omega}_{\mathrm{d}}$, and $\boldsymbol{\omega}_{\mathrm{d}}$ is the desired angular velocity. On the basis of the above definition, the open-loop attitude tracking dynamics can be obtained as[12]

$$\left.\begin{aligned}\dot{\boldsymbol{q}}_{\mathrm{ev}} &= \boldsymbol{Q}\boldsymbol{\omega}_{\mathrm{e}}\\ \dot{\boldsymbol{q}}_{\mathrm{e4}} &= -\frac{1}{2}\boldsymbol{q}_{\mathrm{ev}}^{\mathrm{T}}\boldsymbol{\omega}_{\mathrm{e}}\end{aligned}\right\}, \tag{4}$$

$$\boldsymbol{J}\dot{\boldsymbol{\omega}}_{\mathrm{e}} = -\boldsymbol{\omega}^{\times}\boldsymbol{J}\boldsymbol{\omega} + \boldsymbol{J}\left(\boldsymbol{\omega}_{\mathrm{e}}^{\times}\boldsymbol{C}\boldsymbol{\omega}_{\mathrm{d}} - \boldsymbol{C}\dot{\boldsymbol{\omega}}_{\mathrm{d}}\right) + \boldsymbol{\tau} + \boldsymbol{T}_{\mathrm{d}}, \tag{5}$$

where

$$\begin{aligned}\boldsymbol{Q} &= 0.5\left(\boldsymbol{q}_{\mathrm{ev}}^{\times} + q_{\mathrm{e4}}\boldsymbol{I}_3\right),\\ \boldsymbol{C} &= (q_{\mathrm{e4}}^2 - \boldsymbol{q}_{\mathrm{ev}}^{\mathrm{T}}\boldsymbol{q}_{\mathrm{ev}})\boldsymbol{I}_3 + 2\boldsymbol{q}_{\mathrm{ev}}\boldsymbol{q}_{\mathrm{ev}}^{\mathrm{T}} - 2q_{\mathrm{e4}}\boldsymbol{q}_{\mathrm{ev}}^{\times}\end{aligned}$$

denotes the corresponding rotation matrix satisfying $\|\boldsymbol{C}\| = 1$ and $\dot{\boldsymbol{C}} = -\boldsymbol{\omega}_{\mathrm{e}}^{\times}\boldsymbol{C}$; $\boldsymbol{\omega}_{\mathrm{e}} \in \mathbb{R}^3$ is the relative angular velocity between the body-fixed frame and the inertial reference frame.

In order to facilitate the control law derivation, manipulation of Eqs. (4) and (5) results in[12]

$$\boldsymbol{M}^{*}\ddot{\boldsymbol{q}}_{\mathrm{ev}} + \boldsymbol{N}\dot{\boldsymbol{q}}_{\mathrm{ev}} + \boldsymbol{P}^{\mathrm{T}}\boldsymbol{H} = \boldsymbol{P}^{\mathrm{T}}\left(\boldsymbol{\tau} + \boldsymbol{T}_{\mathrm{d}}\right), \tag{6}$$

where $\boldsymbol{P}$ is the inverse matrix of $\boldsymbol{Q}$,

$$\begin{aligned}\boldsymbol{M}^{*} &= \boldsymbol{P}^{\mathrm{T}}\boldsymbol{J}\boldsymbol{P},\\ \boldsymbol{N} &= \boldsymbol{P}^{\mathrm{T}}\boldsymbol{J}\dot{\boldsymbol{P}} - \boldsymbol{P}^{\mathrm{T}}(\boldsymbol{J}\boldsymbol{P}\dot{\boldsymbol{q}}_{\mathrm{ev}})^{\times}\boldsymbol{P},\\ \boldsymbol{H} &= (\boldsymbol{P}\dot{\boldsymbol{q}}_{\mathrm{ev}})^{\times}\boldsymbol{J}(\boldsymbol{C}\dot{\boldsymbol{\omega}}_{\mathrm{d}}) + (\boldsymbol{C}\boldsymbol{\omega}_{\mathrm{d}})^{\times}\boldsymbol{J}(\boldsymbol{P}\dot{\boldsymbol{q}}_{\mathrm{ev}}) +\\ &\quad (\boldsymbol{C}\boldsymbol{\omega}_{\mathrm{d}})^{\times}\boldsymbol{J}(\boldsymbol{C}\boldsymbol{\omega}_{\mathrm{d}}) - \boldsymbol{J}\boldsymbol{P}(\boldsymbol{\omega}_{\mathrm{e}}^{\times}\boldsymbol{C}\boldsymbol{\omega}_{\mathrm{d}} - \boldsymbol{C}\dot{\boldsymbol{\omega}}_{\mathrm{d}}).\end{aligned}$$

The transformed system has the following properties.

Property 1 $\boldsymbol{M}^{*}$ is symmetric positive definite.

Property 2 The matrix $\boldsymbol{M}^{*} - 2\boldsymbol{N}$ is a skew symmetric satisfying $\boldsymbol{x}^{\mathrm{T}}(\dot{\boldsymbol{M}}^{*} - 2\boldsymbol{N})\boldsymbol{x} = \boldsymbol{0}$ for $\forall \boldsymbol{x} \in \mathbb{R}^3$.

Assumption 1 There exists a positive but unknown scalar $\boldsymbol{J}_{\max}$ such that $\|\boldsymbol{J}\| \leqslant \boldsymbol{J}_{\max}$.

The inertia matrix is time-varying and uncertain due to the fuel consumption and/or the unfolding of solar array and some other factors, but remains positive definite and bounded all the time. Therefore, it is reasonable to assume that $\|\boldsymbol{J}\| \leqslant \boldsymbol{J}_{\max}$.

In this work, we seek to present a finite-time control law for spacecraft attitude tracking maneuvers to achieve the finite-time convergence of the attitude tracking error, in the presence of external disturbances, unknown inertia properties and input saturation.

1.3 Relevant Lemma

The system is considered as

$$\dot{\boldsymbol{x}} = f(\boldsymbol{x}, t), \quad f(0, t) = \boldsymbol{0}, \quad \boldsymbol{x} \in \mathbb{R}^n,$$

where $f : U \to \mathbb{R}^n$ is continuous on an open neighborhood U of the origin. Assume that the above system has a unique solution in forward time for all initial conditions.

Lemma 1[13] For the system mentioned above, given a Lyapunov function $V(x)$, real numbers $\alpha \in (0, 1)$, $c > 0$ and $0 < \eta < \infty$ such that

$$\dot{V}(x) \leqslant -cV^{\alpha}(x) + \eta,$$

then the trajectory of system is practical finite-time stable. And the states of system converge to a residual set described as

$$V^{\alpha}(x) \leqslant \eta c(1-\theta), \quad \forall t \geqslant T$$

in a finite time. The convergence time T is given by

$$T \leqslant \frac{V^{1-\alpha}(x_0)}{\lambda\theta(1-\alpha)},$$

where λ and $0 < \theta < 1$ are positive constants, and $V(x_0)$ is the initial value of V.

Notation Throughout this paper, we use $\|\cdot\|$ for the Euclidean norm of vectors and the induced norm for matrices. For a given vector $\boldsymbol{x} = [x_1 \quad x_2 \quad x_3]^{\mathrm{T}} \in \mathbb{R}^3$, define $\boldsymbol{x}^{\alpha} = [x_1^{\alpha} \quad x_2^{\alpha} \quad x_3^{\alpha}]^{\mathrm{T}}$, $\mathrm{sgn}(\boldsymbol{x}) = [\mathrm{sgn}(x_1) \quad \mathrm{sgn}(x_2) \quad \mathrm{sgn}(x_3)]^{\mathrm{T}}$ and $\mathrm{sig}^{\alpha}(\boldsymbol{x}) = [x_1^{\alpha}\mathrm{sgn}(x_1) \quad x_2^{\alpha}\mathrm{sgn}(x_2) \quad x_3^{\alpha}\mathrm{sgn}(x_3)]^{\mathrm{T}}$, where $\alpha \in \mathbb{R}$.

Lemma 2[14] Considering symmetric and positive matrix $\boldsymbol{B} \in \mathbb{R}^{3\times 3}$, maximum positive constant $\lambda_{\max}$ and minimum positive constant $\lambda_{\min}$, it is bounded as $\lambda_{\min}\|\boldsymbol{x}\|^2 \leqslant \boldsymbol{x}^{\mathrm{T}}\boldsymbol{B}\boldsymbol{x} \leqslant \lambda_{\max}\|\boldsymbol{x}\|^2$, $\forall \boldsymbol{B}$, $\boldsymbol{x} \in \mathbb{R}^3$.

2 Control Law Design and Stability Analysis

With time-varying SMC and adaptive techniques, an adaptive controller is designed to achieve finite-time attitude tracking under input saturation.

For the attitude tracking dynamics, a novel time-varying sliding mode surface is designed as

$$\boldsymbol{s} = [s_1(t) \quad s_2(t) \quad s_3(t)]^{\mathrm{T}} = \dot{\boldsymbol{q}}_{\mathrm{ev}} + k\boldsymbol{q}_{\mathrm{ev}} - \boldsymbol{f}(t), \tag{7}$$

where k is a positive scalar to be determined by designer, and $\boldsymbol{f}(t) = [f_1(t) \quad f_2(t) \quad f_3(t)]^{\mathrm{T}}$ is the forcing function in sliding mode dynamics with its analytical form of

$$\boldsymbol{f}(t) = \begin{cases} \dot{\boldsymbol{q}}_{\mathrm{ev}}(0) + k\boldsymbol{q}_{\mathrm{ev}}(0), & 0 \leqslant t < t_{\mathrm{m}} \\ \left[1 - \rho(1 - \mathrm{e}^{-k(t-t_{\mathrm{m}})})\right](\dot{\boldsymbol{q}}_{\mathrm{ev}}(0) + \\ \quad k\boldsymbol{q}_{\mathrm{ev}}(0))\cos\dfrac{\pi(t-t_{\mathrm{m}})}{2(t_{\mathrm{f}}-t_{\mathrm{m}})}, & t_{\mathrm{m}} \leqslant t < t_{\mathrm{f}} \\ \boldsymbol{0}, & t \geqslant t_{\mathrm{f}} \end{cases}. \tag{8}$$

In Eq. (8), $\dot{\boldsymbol{q}}_{\mathrm{ev}}(0)$ and $\boldsymbol{q}_{\mathrm{ev}}(0)$ refer to the initial values of $\dot{\boldsymbol{q}}_{\mathrm{ev}}$ and $\boldsymbol{q}_{\mathrm{ev}}$, respectively; $\boldsymbol{f}(t)$ is continuous, and its first derivative is 0 or bounded in switch points (this property is a basic requirement for the existence of a sliding control); ρ is constant parameter; t_{f} is the terminal time specified by the designer according to the mission requirement, and system states will reach the sliding manifold within finite time t_{m} using the designed controller. It is obvious that $\boldsymbol{s} = [0 \quad 0 \quad 0]^{\mathrm{T}}$ when $t = 0$.

Lemma 3 Consider the time-varying sliding manifold $\boldsymbol{s}$ defined in Eq. (7). If an effective control law ensures that the state trajectories originating from the sliding regime reach the sliding manifold within t_{m} and hold on it thereafter, then the tracking errors $\dot{\boldsymbol{q}}_{\mathrm{ev}}$ and $\boldsymbol{q}_{\mathrm{ev}}$ converge to zero at the time t_{f}, and for all $t \geqslant t_{\mathrm{f}}$, $\boldsymbol{q}_{\mathrm{ev}} \equiv \boldsymbol{0}$ and $\dot{\boldsymbol{q}}_{\mathrm{ev}} \equiv \boldsymbol{0}$.

Proof If the designed controller ensures $\boldsymbol{s}$ to be zero within finite time t_{m} and stays zero for all $t \geqslant t_{\mathrm{m}}$, it follows that

$$\dot{\boldsymbol{q}}_{\mathrm{ev}} + k\boldsymbol{q}_{\mathrm{ev}} = \boldsymbol{f}(t), \quad \forall t \geqslant t_{\mathrm{m}}. \tag{9}$$

For $t \geqslant t_{\mathrm{m}}$, the tracking error and sliding mode surface $\boldsymbol{s}$ need to be verified in two separate periods. To show the convergence of $\dot{\boldsymbol{q}}_{\mathrm{ev}} + k\boldsymbol{q}_{\mathrm{ev}}$, we first analyze the response in time interval $t_{\mathrm{m}} < t \leqslant t_{\mathrm{f}}$.

For $t_{\mathrm{m}} < t \leqslant t_{\mathrm{f}}$, solving Eqs. (8) and (9) yields

$$\boldsymbol{q}_{\mathrm{ev}}(t)\mathrm{e}^{kt}\Big|_{t_{\mathrm{m}}}^{t} = (1-\rho)\boldsymbol{p}_1\int_{t_{\mathrm{m}}}^{t}\mathrm{e}^{k\tau}\cos\frac{\pi(t-t_{\mathrm{m}})}{2(t_{\mathrm{f}}-t_{\mathrm{m}})}\mathrm{d}\tau + \rho\mathrm{e}^{kt_{\mathrm{m}}}\boldsymbol{p}_1\int_{t_{\mathrm{m}}}^{t}\cos\frac{\pi(t-t_{\mathrm{m}})}{2(t_{\mathrm{f}}-t_{\mathrm{m}})}\mathrm{d}\tau,$$

where $\boldsymbol{p}_1 = \dot{\boldsymbol{q}}_{\mathrm{ev}}(0) + k\boldsymbol{q}_{\mathrm{ev}}(0)$. Then, the expression of $\boldsymbol{q}_{\mathrm{ev}}(t)$ from t_{m} to t_{f} can be obtained as

$$\begin{aligned}\boldsymbol{q}_{\mathrm{ev}}(t) = {} & \boldsymbol{q}_{\mathrm{ev}}(0)\mathrm{e}^{-k(t-t_m)} + \frac{1}{p}\Big[(1-\rho)\boldsymbol{p}_1 k\cos\frac{\pi(t-t_{\mathrm{m}})}{2(t_{\mathrm{f}}-t_{\mathrm{m}})} + \\ & \frac{(1-\rho)\boldsymbol{p}_1\pi}{2(t_{\mathrm{f}}-t_{\mathrm{m}})}\sin\frac{\pi(t-t_{\mathrm{m}})}{2(t_{\mathrm{f}}-t_{\mathrm{m}})} - \\ & (1-\rho)\boldsymbol{p}_1 k\mathrm{e}^{-k(t-t_{\mathrm{m}})}\Big] + \\ & 2\rho\mathrm{e}^{-k(t-t_{\mathrm{m}})}\boldsymbol{p}_1(t_{\mathrm{f}}-t_{\mathrm{m}})\frac{1}{\pi}\sin\frac{\pi(t-t_{\mathrm{m}})}{2(t_{\mathrm{f}}-t_{\mathrm{m}})},\end{aligned}$$

where $p = k^2 + \dfrac{\pi}{2(t_{\mathrm{f}}-t_{\mathrm{m}})}$. In order to ensure $\boldsymbol{q}_{\mathrm{ev}}(t) = \boldsymbol{0}$ when $t = t_{\mathrm{f}}$, the constant ρ in the forcing function can be resolved as

$$\rho = \frac{\boldsymbol{q}_{\mathrm{ev}}(0)\mathrm{e}^{-k(t_{\mathrm{f}}-t_{\mathrm{m}})} + \dfrac{\boldsymbol{p}_1\mathrm{e}^{-kt_{\mathrm{f}}}\pi}{2p(t_{\mathrm{f}}-t_{\mathrm{m}})} - \dfrac{\boldsymbol{p}_1 k\mathrm{e}^{kt_{\mathrm{m}}}}{p}}{\dfrac{\boldsymbol{p}_1\mathrm{e}^{kt_{\mathrm{f}}}\pi}{2(t_{\mathrm{f}}-t_{\mathrm{m}})} - \dfrac{\boldsymbol{p}_1 k\mathrm{e}^{kt_{\mathrm{m}}}}{p} - \dfrac{2\mathrm{e}^{-k(t_{\mathrm{f}}-t_{\mathrm{m}})}\boldsymbol{p}_1(t_{\mathrm{f}}-t_{\mathrm{m}})}{\pi}}. \tag{10}$$

With the choice of constant parameter ρ calculated in Eq. (10), the sliding mode manifold can force $\boldsymbol{q}_{\mathrm{ev}}(t_{\mathrm{f}}) = \mathbf{0}$. Further, the response of $\dot{\boldsymbol{q}}_{\mathrm{ev}}(t)$ at the time $t = t_{\mathrm{f}}$ needs to be verified; obviously, $\dot{\boldsymbol{q}}_{\mathrm{ev}}(t)$ can be obtained as $\dot{\boldsymbol{q}}_{\mathrm{ev}}(t_{\mathrm{f}}) = \mathbf{0}$ corresponding to $\dot{\boldsymbol{q}}_{\mathrm{ev}}(t_{\mathrm{f}}) + k\boldsymbol{q}_{\mathrm{ev}}(t_{\mathrm{f}}) = \boldsymbol{f}(t_{\mathrm{f}}) = \mathbf{0}$. Then, solving Eq. (9) we can obtain $\dot{\boldsymbol{q}}_{\mathrm{ev}}(t) = \mathbf{0}$ and $\boldsymbol{q}_{\mathrm{ev}}(t) = \mathbf{0}$ with the continuity of $\boldsymbol{q}_{\mathrm{ev}}(t)$ and $\lim\limits_{t\to t_{\mathrm{f}}} \boldsymbol{q}_{\mathrm{ev}}(t) = \mathbf{0}$ for $t > t_{\mathrm{f}}$. Hence, $\boldsymbol{q}_{\mathrm{ev}}(t) \equiv \mathbf{0}$ and $\dot{\boldsymbol{q}}_{\mathrm{ev}}(t) \equiv \mathbf{0}$ can be gained for all $t \geqslant t_{\mathrm{f}}$ with the above indication, that is, we conclude the finite-time convergence. Then proof is completed.

Remark 1 Compared with other time-varying sliding mode surfaces, the forcing function $\boldsymbol{f}(t)$ can guarantee the finite-time convergence of the system states to equilibrium point.

In order to design the finite-time fault-tolerant attitude tracking controller, an auxiliary tracking error is introduced as[15]

$$\boldsymbol{e}_{\mathrm{r}} = \boldsymbol{s} - \dot{\boldsymbol{q}}_{\mathrm{ev}}. \tag{11}$$

By Eqs. (6) and (11), the open-loop dynamics of $\boldsymbol{s}$ can be defined as

$$\boldsymbol{M}\dot{\boldsymbol{s}} + \boldsymbol{C}\boldsymbol{s} = \boldsymbol{P}^{\mathrm{T}}\boldsymbol{\tau} + \boldsymbol{P}^{\mathrm{T}}\boldsymbol{d} + \boldsymbol{R}, \tag{12}$$

where the variable $\boldsymbol{d} = \bar{\boldsymbol{u}} + \boldsymbol{T}_{\mathrm{d}}$ is the total interference; $\boldsymbol{R} = \boldsymbol{M}^{*}\dot{\boldsymbol{e}}_{\mathrm{r}} + \boldsymbol{C}\boldsymbol{e}_{\mathrm{r}} - \boldsymbol{P}^{\mathrm{T}}\boldsymbol{H}$, and it can be transformed as

$$\boldsymbol{R} = \boldsymbol{P}^{\mathrm{T}}\boldsymbol{Y}(\cdot)\boldsymbol{\theta}. \tag{13}$$

In Eq. (13), $\boldsymbol{\theta} \in \mathbb{R}^6$ is a constant vector defined as $\boldsymbol{\theta} = [J_{11} \;\; J_{13} \;\; J_{13} \;\; J_{22} \;\; J_{23} \;\; J_{33}]^{\mathrm{T}}$ with J_{ij} being the element of $\boldsymbol{J}$; $\boldsymbol{Y}(\cdot) \in \mathbb{R}^{3\times 6}$ is the known regression matrix:

$$\begin{aligned}\boldsymbol{Y}(\cdot) = {} & L(\boldsymbol{P}\dot{\boldsymbol{e}}_{\mathrm{r}}) + L(\dot{\boldsymbol{P}}\boldsymbol{e}_{\mathrm{r}}) + (\boldsymbol{P}\boldsymbol{e}_{\mathrm{r}})^{\times}L(\boldsymbol{\omega}_{\mathrm{e}}) - \\ & \boldsymbol{\omega}_{\mathrm{e}}^{\times}L(\boldsymbol{C}\boldsymbol{\omega}_{\mathrm{d}}) - (\boldsymbol{C}\boldsymbol{\omega}_{\mathrm{d}})^{\times}L(\boldsymbol{\omega}_{\mathrm{e}} + \boldsymbol{C}\boldsymbol{\omega}_{\mathrm{d}}) + \\ & L(\boldsymbol{\omega}_{\mathrm{e}}^{\times}\boldsymbol{C}\boldsymbol{\omega}_{\mathrm{d}} - \boldsymbol{C}\dot{\boldsymbol{\omega}}_{\mathrm{d}}),\end{aligned}$$

where $L(\cdot)$ is an operator defined by

$$L(\boldsymbol{x}) = \begin{bmatrix} x_1 & x_2 & x_3 & 0 & 0 & 0 \\ 0 & x_1 & 0 & x_2 & x_3 & 0 \\ 0 & 0 & x_1 & 0 & x_2 & x_3 \end{bmatrix}.$$

In Eq. (12), $\boldsymbol{P}^{\mathrm{T}}\boldsymbol{d} + \boldsymbol{R}$ denotes an uncertainty function containing external disturbances and uncertainty of system.

Considering actuator input constraints, the control torque $\boldsymbol{\tau} = [\tau_1 \;\; \tau_2 \;\; \tau_3]$ has an upper limit and a lower limit. Hence, the control law is designed as

$$\boldsymbol{u} = \mathrm{sat}(\boldsymbol{v}, u_{\max}),$$

where, $\boldsymbol{v}$ is the input signal of controller; $u_{\max} = \tau_{\max}$ is a known constant which is the maximum torque the actuator can produce; $\mathrm{sat}(\boldsymbol{v}, u_{\max})$ denotes the nonlinear saturation characteristic of the actuator and is of the form as $\mathrm{sat}(u_i) = \mathrm{sgn}(u_i)\min\{|u_i|, u_{\max}\}$ for $i = 1, 2, 3$.

For convenience of input constraint effect analysis, the auxiliary design system is given by

$$\dot{\boldsymbol{x}}_{\mathrm{a}} = -\boldsymbol{x}_{\mathrm{a}}\frac{(\boldsymbol{P}\boldsymbol{s})^{\mathrm{T}}\Delta\boldsymbol{u}}{\|\boldsymbol{x}_{\mathrm{a}}\|^2} - k_2\boldsymbol{x}_{\mathrm{a}} - k_5\mathrm{sig}^r(\boldsymbol{x}_{\mathrm{a}}), \tag{14}$$

where

$$\Delta\boldsymbol{u} = \boldsymbol{u} - \boldsymbol{v},$$

k_2, k_5 and r are positive scalars to be designed; $\boldsymbol{x}_{\mathrm{a}} \in \mathbb{R}^3$ is the state of the auxiliary design system.

Note that introduction of proceeding auxiliary system is to handle input saturation. The auxiliary system designed in Eq. (14) is presented to analyze the effect of saturation constraint, and auxiliary $\boldsymbol{x}_{\mathrm{a}}$ is used to design the following control law to help in providing stability analysis to the closed-loop attitude system.

Theorem 1 Consider the attitude tracking control system given in Eq. (6). The control law $\boldsymbol{u}$ implemented with $\boldsymbol{v}$ and the updating law are firstly designed as

$$\begin{aligned}\boldsymbol{v} = {} & -k_1\mathrm{sig}^r(\boldsymbol{P}\boldsymbol{s}) - \hat{\boldsymbol{b}}\boldsymbol{\varphi}\mathrm{sgn}(\boldsymbol{P}\boldsymbol{s}) - \\ & k_3(\boldsymbol{P}\boldsymbol{s}) - k_4\boldsymbol{x}_a,\end{aligned} \tag{15}$$

$$\dot{\hat{\boldsymbol{b}}} = \delta_1(\boldsymbol{\varphi}\|\boldsymbol{P}\boldsymbol{s}\| - \lambda_1\hat{\boldsymbol{b}}), \tag{16}$$

where k_1, k_3, k_4, δ_1 and λ_1 are positive control gains, and $\boldsymbol{\varphi} = [\|\boldsymbol{Y}(\cdot)\|_{\mathrm{F}} \;\; 1]$; the adaptive value $\hat{\boldsymbol{b}}$ is the estimate of the unknown parameter $\boldsymbol{b}$, $\boldsymbol{b} = [\|\boldsymbol{\theta}\| \;\; d_{\mathrm{m}}]$, and d_{m} is the upper bound of disturbance $\boldsymbol{d}$ (it is time-invariant but unknown scalar). Suppose that the control parameters are chosen such that

$$k_3 > 0.5, \quad k_2 > 0.5k_4^2.$$

If controller parameters are chosen properly such that the system states reach the sliding manifold in a finite time t_{m}, then the finite-time convergence of relative tracking error is achieved as $\boldsymbol{q}_{\mathrm{ev}} \equiv \mathbf{0}$ for $t > t_{\mathrm{f}}$.

Proof Consider the following Lyapunov function candidate:

$$V_1 = 0.5\boldsymbol{s}^{\mathrm{T}}\boldsymbol{M}^{*}\boldsymbol{s} + \frac{1}{2\delta_1}\tilde{\boldsymbol{b}}^{\mathrm{T}}\tilde{\boldsymbol{b}} + 0.5\boldsymbol{x}_{\mathrm{a}}^{\mathrm{T}}\boldsymbol{x}_{\mathrm{a}}, \tag{17}$$

where $\tilde{\boldsymbol{b}} = \boldsymbol{b} - \hat{\boldsymbol{b}}$. Taking the time derivative of V_1 leads to

$$\dot{V}_1 = \boldsymbol{s}^{\mathrm{T}}\boldsymbol{P}^{\mathrm{T}}\boldsymbol{v} + \boldsymbol{s}^{\mathrm{T}}\boldsymbol{P}^{\mathrm{T}}(\boldsymbol{d} + \boldsymbol{R}) - \frac{1}{\delta_1}\tilde{\boldsymbol{b}}^{\mathrm{T}}\dot{\hat{\boldsymbol{b}}} + \boldsymbol{x}_{\mathrm{a}}^{\mathrm{T}}\dot{\boldsymbol{x}}_{\mathrm{a}}. \tag{18}$$

Applying Assumption 1, Property 1, Property 2, Lemma 2 and Eq. (15) yields

$$\begin{aligned}\dot{V} = {} & \boldsymbol{s}^{\mathrm{T}}\boldsymbol{P}^{\mathrm{T}}\Big(-k_1\mathrm{sig}^r(\boldsymbol{P}\boldsymbol{s}) - \hat{\boldsymbol{b}}\boldsymbol{\varphi}\mathrm{sgn}(\boldsymbol{P}\boldsymbol{s}) - \\ & k_3(\boldsymbol{P}\boldsymbol{s}) - k_4\boldsymbol{x}_{\mathrm{a}}\Big) + \boldsymbol{s}^{\mathrm{T}}\boldsymbol{P}^{\mathrm{T}}(\boldsymbol{d} + \boldsymbol{R}) -\end{aligned}$$

$$\frac{1}{\delta_1}\tilde{\boldsymbol{b}}^{\mathrm{T}}\dot{\hat{\boldsymbol{b}}}+\boldsymbol{x}_{\mathrm{a}}^{\mathrm{T}}\dot{\boldsymbol{x}}_{\mathrm{a}}+\boldsymbol{s}^{\mathrm{T}}\boldsymbol{P}^{\mathrm{T}}\Delta\boldsymbol{u}\leqslant$$
$$-k_1\|\boldsymbol{Ps}\|^{1+r}-\boldsymbol{s}^{\mathrm{T}}\boldsymbol{P}^{\mathrm{T}}\hat{\boldsymbol{b}}\boldsymbol{\varphi}\mathrm{sgn}(\boldsymbol{Ps})-k_3\|\boldsymbol{Ps}\|^2-$$
$$k_4\boldsymbol{s}^{\mathrm{T}}\boldsymbol{P}^{\mathrm{T}}\boldsymbol{x}_{\mathrm{a}}+\|\boldsymbol{Ps}\|^2(\boldsymbol{d}+\boldsymbol{R})-$$
$$\frac{1}{\delta_1}\tilde{\boldsymbol{b}}^{\mathrm{T}}\Big(\delta_1\boldsymbol{\varphi}\|\boldsymbol{Ps}\|-\lambda_1\hat{\boldsymbol{b}}\Big)+$$
$$\boldsymbol{x}_{\mathrm{a}}^{\mathrm{T}}\Big(-\boldsymbol{x}_{\mathrm{a}}\frac{(\boldsymbol{Ps})^{\mathrm{T}}\Delta\boldsymbol{u}}{\|\boldsymbol{x}_{\mathrm{a}}\|^2}-k_2\boldsymbol{x}_{\mathrm{a}}-k_5\mathrm{sig}^r(\boldsymbol{x}_{\mathrm{a}})\Big)+$$
$$\boldsymbol{s}^{\mathrm{T}}\boldsymbol{P}^{\mathrm{T}}\Delta\boldsymbol{u}\leqslant$$
$$-k_1\|\boldsymbol{Ps}\|^{1+r}+$$
$$(\boldsymbol{b}-\hat{\boldsymbol{b}})^{\mathrm{T}}\boldsymbol{\varphi}\,\|\boldsymbol{Ps}\|-k_3\|\boldsymbol{Ps}\|^2-k_4\boldsymbol{s}^{\mathrm{T}}\boldsymbol{P}^{\mathrm{T}}\boldsymbol{x}_{\mathrm{a}}-$$
$$\tilde{\boldsymbol{b}}^{\mathrm{T}}\boldsymbol{\varphi}\|\boldsymbol{Ps}\|+\lambda_1\tilde{\boldsymbol{b}}^{\mathrm{T}}\hat{\boldsymbol{b}}-k_2\|\boldsymbol{x}_{\mathrm{a}}\|^2-k_5\|\boldsymbol{x}_{\mathrm{a}}\|^{1+r}-$$
$$k_4(\boldsymbol{Ps})^{\mathrm{T}}\boldsymbol{x}_{\mathrm{a}},$$

so $-k_4(\boldsymbol{Ps})^{\mathrm{T}}\boldsymbol{x}_{\mathrm{a}}$ can be established by using Young's inequality:

$$-k_4(\boldsymbol{Ps})^{\mathrm{T}}\boldsymbol{x}_{\mathrm{a}}\leqslant\frac{1}{2}\|\boldsymbol{Ps}\|^2+\frac{k_4^2}{2}\|\boldsymbol{x}_{\mathrm{a}}\|^2.$$

It follows that

$$\begin{aligned}\dot{V}\leqslant&-k_1\|\boldsymbol{Ps}\|^{1+r}+\lambda_1\tilde{\boldsymbol{b}}^{\mathrm{T}}\hat{\boldsymbol{b}}-k_3\|\boldsymbol{Ps}\|^2-\\&k_2\|\boldsymbol{x}_{\mathrm{a}}\|^2-k_5\|\boldsymbol{x}_{\mathrm{a}}\|^{1+r}-k_4(\boldsymbol{Ps})^{\mathrm{T}}\boldsymbol{x}_{\mathrm{a}}\leqslant\\&-k_1\|\boldsymbol{Ps}\|^{1+r}+\lambda_1\tilde{\boldsymbol{b}}^{\mathrm{T}}\hat{\boldsymbol{b}}-k_3\|\boldsymbol{Ps}\|^2-\\&k_2\|\boldsymbol{x}_{\mathrm{a}}\|^2-k_5\|\boldsymbol{x}_{\mathrm{a}}\|^{1+r}+0.5\|\boldsymbol{Ps}\|^2+\frac{k_4^2}{2}\|\boldsymbol{x}_{\mathrm{a}}\|^2\leqslant\\&-k_1\|\boldsymbol{Ps}\|^{1+r}-(k_3-0.5)\|\boldsymbol{Ps}\|^2-\\&\Big(k_2-\frac{k_4^2}{2}\Big)\|\boldsymbol{x}_{\mathrm{a}}\|^2-k_5\|\boldsymbol{x}_{\mathrm{a}}\|^{1+r}+\lambda_1\tilde{\boldsymbol{b}}^{\mathrm{T}}\hat{\boldsymbol{b}}.\end{aligned}$$

For $\forall\gamma\in(0.5,1)$, the term $\lambda_1\tilde{\boldsymbol{b}}_i^{\mathrm{T}}\hat{\boldsymbol{b}}_i$, $i=1,\,2$, satisfies

$$\begin{aligned}\lambda_1\tilde{\boldsymbol{b}}_i^{\mathrm{T}}\hat{\boldsymbol{b}}_i=&-\lambda_1\tilde{\boldsymbol{b}}_i^{\mathrm{T}}(\tilde{\boldsymbol{b}}_i-\boldsymbol{b}_i)\leqslant-\upsilon[(\tilde{\boldsymbol{b}}_i)^2]^{(1+\kappa)/2}+\\&\left[\frac{\lambda_1(2\gamma-1)(\tilde{\boldsymbol{b}}_i)^2}{2\gamma}\right]^{(1+\kappa)/2}-\\&\frac{\lambda_1(2\gamma-1)}{2\gamma}(\tilde{\boldsymbol{b}}_i)^2+\frac{\gamma\lambda_1}{2}(\boldsymbol{b}_i)^2,\end{aligned}$$

where $\upsilon=\Big(\lambda_1\dfrac{2\gamma-1}{2\gamma}\Big)^{(1+\kappa)/2}$ and $\kappa\in(0,1)$.

Two cases are considered to further deal with the above inequality.

Case 1 If

$$\frac{\lambda_1(2\gamma-1)}{2\gamma}\Big(\tilde{\boldsymbol{b}}_i\Big)^2\geqslant\boldsymbol{1},$$

it is obvious that

$$\underbrace{\left[\frac{\lambda_1(2\gamma-1)}{2\gamma}(\tilde{\boldsymbol{b}}_i)^2\right]^{(1+\kappa)/2}-\frac{\lambda_1(2\gamma-1)}{2\gamma}(\tilde{\boldsymbol{b}}_i)^2}_{\chi}\leqslant\boldsymbol{0}$$

holds, due to $0.75<(1+\kappa)/2<1$.

Case 2 If

$$\frac{\lambda_1(2\gamma-1)}{2\gamma}(\tilde{\boldsymbol{b}}_i)^2<\boldsymbol{1},$$

in terms of the characteristic of a power function, the term χ is bounded within a certain range of $[0,\rho]$, with $\rho\leqslant1$.

Hence, we can easily get

$$\begin{aligned}\lambda_1\tilde{\boldsymbol{b}}^{\mathrm{T}}\hat{\boldsymbol{b}}\leqslant&-\upsilon\sum_{i=1}^{2}[(\tilde{\boldsymbol{b}})^2]^{(1+\kappa)/2}+3\rho+0.5\lambda_1\gamma\boldsymbol{b}^{\mathrm{T}}\boldsymbol{b}\leqslant\\&-\upsilon(\tilde{\boldsymbol{b}}^{\mathrm{T}}\tilde{\boldsymbol{b}})^{(1+\kappa)/2}+3\rho+0.5\lambda_1\gamma\boldsymbol{b}^{\mathrm{T}}\boldsymbol{b}.\end{aligned}$$

Let $\kappa=r$ and suppose that the control parameters are chosen such that

$$k_3>\frac{1}{2},\quad k_2>\frac{k_4^2}{2}.$$

Then, we can easily get

$$\begin{aligned}\dot{V}\leqslant&-k_1\|\boldsymbol{Ps}\|^{1+r}-\upsilon(\tilde{\boldsymbol{b}}^{\mathrm{T}}\tilde{\boldsymbol{b}})^{(1+r)/2}+\\&3\rho+0.5\lambda_1\gamma\boldsymbol{b}^{\mathrm{T}}\boldsymbol{b}-k_5\|\boldsymbol{x}_{\mathrm{a}}\|^{1+r}\leqslant\\&\sqrt[(1+r)/2]{2/\lambda_{\max}(\boldsymbol{J})}k_1(0.5\boldsymbol{s}^{\mathrm{T}}\boldsymbol{M}^*\boldsymbol{s})^{(1+r)/2}-\\&\sqrt[(1+r)/2]{2\delta_1}\upsilon\left(\frac{1}{2\delta_1}\tilde{\boldsymbol{b}}^{\mathrm{T}}\tilde{\boldsymbol{b}}\right)^{(1+r)/2}-\\&\sqrt[(1+r)/2]{2}k_5(0.5\boldsymbol{x}_{\mathrm{a}}^{\mathrm{T}}\boldsymbol{x}_{\mathrm{a}})^{(1+r)/2}\leqslant\\&-cV^{(1+r)/2}+\eta,\end{aligned}$$

where

$$c=\min\left\{\sqrt[(1+r)/2]{2/\lambda_{\max}(\boldsymbol{J})}k_1,\ \sqrt[(1+r)/2]{\delta}\upsilon,\ \sqrt[(1+r)/2]{2}k_5\right\},$$
$$\eta=3\rho+0.5\lambda_1\gamma\boldsymbol{b}^{\mathrm{T}}\boldsymbol{b},$$

$\lambda_{\max}(\boldsymbol{J})$ is the maximum eigenvalue of $\boldsymbol{J}$.

It is then concluded from Lemma 1 that V_1 is finite-time stable and converges to the origin satisfying

$$V^{(1+r)/2}\leqslant\eta/(1-\theta_0)\beta_1,$$

where $\theta_0\in(0,1]$, β_1 is a positive scalar.

A time variable is given by

$$T_{\mathrm{reach}}\leqslant\frac{V^{\frac{1-r}{2}}(x_0)}{\beta_1\theta_0\dfrac{1-r}{2}}.$$

Based on the above analysis and the properties of sliding mode manifold, it can be concluded that: if the residual set is sufficiently small, $V(t)$ can be approximately defined as $V(t)\equiv0$ for all $t\geqslant T_{\mathrm{reach}}$; if we choose proper t_{m} such that $t_{\mathrm{m}}\geqslant T_{\mathrm{reach}}$, the tracking error vector will converge to equilibrium point within specified time t_{f}, and it is designed according to mission requirement, that is, $\lim\limits_{t\to t_{\mathrm{f}}} \boldsymbol{q}_{\mathrm{ev}} = \boldsymbol{0}$, $\lim\limits_{t\to t_{\mathrm{f}}} \dot{\boldsymbol{q}}_{\mathrm{ev}} = \boldsymbol{0}$. Hence, we have completed the proof of Theorem 1.

Remark 2 In this paper, there exists a singularity problem for the proposed controller in auxiliary system Eq. (14) when $\boldsymbol{x}_{\mathrm{a}} = \boldsymbol{0}$. Considering that all of the trajectories of the closed-loop attitude system are practical finite-time stable, the auxiliary system is modified to overcome the singularity problem:

$$\boldsymbol{x}_{\mathrm{a}} = -\boldsymbol{x}_{\mathrm{a}}\frac{(\boldsymbol{Ps})^{\mathrm{T}}\Delta\boldsymbol{u}}{\|\boldsymbol{x}_{\mathrm{a}}\|^2+\varepsilon} - k_2\boldsymbol{x}_{\mathrm{a}} - k_5\mathrm{sig}^r(\boldsymbol{x}_{\mathrm{a}}),$$

where ε is a small positive scalar.

3 Numerical Simulation

Numerical simulation is carried out to demonstrate the effectiveness of the proposed control scheme. The inertia matrix is set as $\boldsymbol{J} = \begin{bmatrix} 20 & 0 & 0 \\ 0 & 17 & 0 \\ 0 & 0 & 15 \end{bmatrix}$ $\mathrm{kg}\cdot\mathrm{m}^2$; the products of inertia are small than $0.5\,\mathrm{kg}\cdot\mathrm{m}^2$; $\Delta\boldsymbol{J} = \mathrm{diag}(1, 1.5, 1.5)\,\mathrm{kg}\cdot\mathrm{m}^2$, $u_{\max} = 0.2\,\mathrm{N}\cdot\mathrm{m}$.

The external disturbance is given as[16]

$$\boldsymbol{d} = 10^{-4}\begin{bmatrix} 3\cos(10\omega_0 t) + 4\sin(3\omega_0 t) - 10 \\ 3\cos(5\omega_0 t) - 1.5\sin(2\omega_0 t) + 15 \\ 3\sin(10\omega_0 t) - 8\sin(4\omega_0 t) + 10 \end{bmatrix}\ \mathrm{N}\cdot\mathrm{m},$$

where $\omega_0 = 0.1$. The maximum allowable control force $F_{\max} = 1\,\mathrm{N}$ is assumed to impose on the actuators. The initial condition is set as $\boldsymbol{q}_{\mathrm{ev}}(0) = [-0.2 \quad 0.5 \quad 0.1 \quad \sqrt{0.7}]^{\mathrm{T}}$, with initial $\boldsymbol{\omega}_{\mathrm{e}}(0) = [-0.02 \ \ 0.01 \ \ 0.02]^{\mathrm{T}}$.

The control parameters are chosen as

$$k_1 = 1, \quad k_2 = 2, \quad k_3 = 1.5, \quad k_4 = 1, \quad k_5 = 2,$$
$$t_{\mathrm{m}} = 30\,\mathrm{s}, \quad t_{\mathrm{f}} = 180\,\mathrm{s}, \quad r = 0.9, \quad \delta_1 = 2, \quad \lambda_1 = 0.1.$$

Time responses of attitude tracking error and angular velocity error are shown in Figs. 1 and 2, respectively. It is observed that, by implementing the proposed controller, the attitude tracking mission is achieved at $t = 180\,\mathrm{s}$ as determined in the controller, that is, the attitude errors and angular velocity errors converge to zero at t_{f}. Meanwhile, angular velocity errors converge to zero rapidly. Although actuators are faulty, the desired target is guaranteed. The steady errors of angular velocity are less than $2\times10^{-5}\,\mathrm{rad/s}$.

Furthermore, the time response of control torque of actuator is shown in Fig. 3 which has interferences and actuator magnitude constraints. Hence, the proposed finite-time controller is not only robust against external disturbances and adaptive to unknown inertia properties, but also able to account for input saturation.

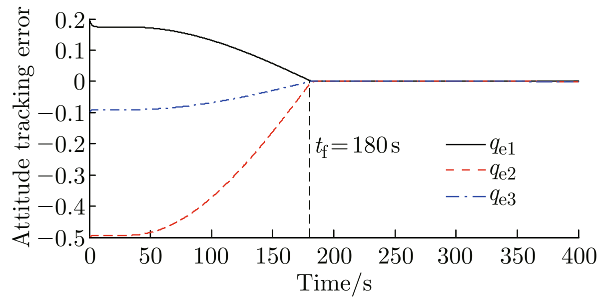

Fig. 1 Time response of attitude tracking error

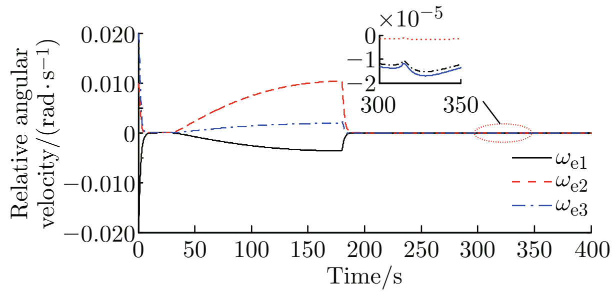

Fig. 2 Time response of angular velocity error

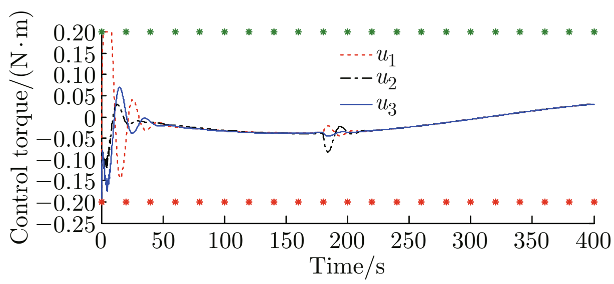

Fig. 3 Time response of control torque of actuator

4 Conclusion

In this paper, an adaptive attitude tracking control strategy has been presented for a rigid spacecraft with an unknown inertia matrix. The proposed control scheme is capable of guaranteeing that the attitude tracking error can converge to equilibrium point within a certain finite time which can be specified a priori by the designer according to specific mission requirements. Moreover, it is proven that the control algorithm developed is not only robust against the external disturbances and adaptive to the unknown inertia properties, but also able to accommodate the saturation nonlinearities simultaneously. The effectiveness of the proposed control scheme is further illustrated by the numerical simulation.

References

[1] YOON H, AGRAWAL B N. Adaptive control of uncertain hamiltonian multi-input multi-output systems:

With application to spacecraft control [J]. *IEEE Transactions on Control Systems Technology*, 2009, **17**(4): 900-906.

[2] LU K F, XIA Y Q, ZHU Z, et al. Sliding mode attitude tracking of rigid spacecraft with disturbances [J]. *Journal of the Franklin Institute*, 2012, **349**(2): 413-440.

[3] ZHANG J H, XIA Y Q. Design of static output feedback sliding mode control for uncertain linear systems [J]. *IEEE Transactions on Industrial Electronics*, 2010, **57**(6): 2161-2170.

[4] LUO W C, CHU Y C, LING K V. H_∞ inverse optimal attitude-tracking control of rigid spacecraft [J]. *Journal of Guidance, Control, and Dynamics*, 2012, **28**(3): 481-494.

[5] JIN E D, SUN Z W. Robust controllers design with finite time convergence for rigid spacecraft attitude tracking control [J]. *Aerospace Science and Technology*, 2008, **12**(4): 324-330.

[6] ZOU A M, KUMAR K D, HOU Z G, et al. Finite-time attitude tracking control for spacecraft using terminal sliding mode and Chebyshev neural network [J]. *IEEE Transactions on Systems, Man, and Cybernetics, Part B: Cybernetics*, 2011, **41**(4): 950-963.

[7] FORBES J R. Attitude control with active actuator saturation prevention [J]. *Acta Astronautica*, 2015, **107**: 187-195.

[8] WIE B, LU J B. Feedback control logic for spacecraft eigenaxis rotations under slew rate and control constraints [J]. *Journal of Guidance, Control, and Dynamics*, 1995, **18**(6): 1372-1379.

[9] BOŠKOVIĆ J D, LI S M, MEHRA R K. Robust tracking control design for spacecraft under control input saturation [J]. *Journal of Guidance, Control, and Dynamics*, 2004, **27**(4): 627-633.

[10] TSIOTRAS P, LUO J H. Control of underactuated spacecraft with bounded inputs [J]. *Automatica*, 2000, **36**(8): 1153-1169.

[11] HU Q L. Variable structure maneuvering control with time-varying sliding surface and active vibration damping of flexible spacecraft with input saturation [J]. *Acta Astronautica*, 2009, **64**(11): 1085-1108.

[12] CAI W C, LIAO X H, SONG Y D. Indirect robust adaptive fault-tolerant control for attitude tracking of spacecraft [J]. *Journal of Guidance, Control, and Dynamics*, 2008, **31**(5): 1456-1463.

[13] XIAO B, HU Q L, ZHANG Y M, et al. Fault-tolerant tracking control of spacecraft with attitude-only measurement under actuator failures [J]. *Journal of Guidance, Control, and Dynamics*, 2014, **37**(3): 838-849.

[14] ZHU Z, XIA Y Q, FU M Y. Attitude stabilization of rigid spacecraft with finite-time convergence [J]. *International Journal of Robust and Nonlinear Control*, 2011, **21**(6): 686-702.

[15] LU K F, XIA Y Q. Adaptive attitude tracking control for rigid spacecraft with finite-time convergence [J]. *Automatica*, 2013, **49**(12): 3591-3599.

[16] XIAO B, HU Q L, ZHANG Y M. Finite-time attitude tracking of spacecraft with fault-tolerant capability [J]. *IEEE Transactions on Control System Technology*, 2015, **23**(4): 1138-1150.